PROCEEDINGS OF SCIENCE

Simulation Status of the Top and Bottom Counting Detectors for the ISS-CREAM Experiment

S.C. Kang[*†1], **Y. Amare**[2], **T. Anderson**[3], **D. Angelaszek**[2,4], **N. Anthony**[4], **K. Cheryian**[4], **G.H. Choi**[5], **M. Copley**[2], **S. Coutu**[3], **L. Derome**[6], **L. Eraud**[6], **L. Hagenau**[4], **J.H. Han**[2], **H.G. Huh**[2], **Y.S. Hwang**[1‡], **H.J. Hyun**[1§], **S. Im**[3], **H.B. Jeon**[1], **J.A. Jeon**[5], **S. Jeong**[5], **H.J. Kim**[1], **K.C. Kim**[2], **M.H. Kim**[2], **H.Y. Lee**[5], **J. Lee**[5], **M.H. Lee**[2], **J. Liang**[4], **J.T. Link**[7], **L. Lu**[4], **L. Lutz**[2], **A. Mechaca-Rocha**[8], **T. Mernik**[2], **J.W. Mitchell**[7], **S.I. Mognet**[3], **S. Morton**[4], **M. Nester**[4], **S. Nutter**[9], **O. Ofoha**[2], **H. Park**[1], **I.H. Park**[5], **J.M. Park**[1¶], **N. Picot-Clemente**[2], **R. Quinn**[4], **E.S. Seo**[2,4], **J.R. Smith**[2], **P. Walpole**[2], **R.P. Weinmann**[2], **J. Wu**[2], **Y.S. Yoon**[2]

1 *Dept. of Physics, Kyungpook National University, Daegu 702-701, Republic of Korea*
2 *Inst. for Phys. Sci. and Tech., University of Maryland, College Park, MD 20742, USA*
3 *Dept. of Physics, Penn State University, University Park, PA 16802, USA*
4 *Dept. of Physics, University of Maryland, College Park, MD 20742, USA*
5 *Dept. of Physics, Sungkyunkwan University, Suwon 440-746, Republic of Korea*
6 *Laboratoire de Physique Subatomique et de Cosmologie, UJF - CNRS/IN2P3 - INP,53 rue des Martyrs, 38026 Grenoble Cedex, France*
7 *Astroparticle Physics Laboratory, NASA Goddard Space Flight Center, Greenbelt, MD 20771, USA*
8 *Instituto de Fisica, Universidad Nacional Autonoma de Mexico, Circuito de la Investigation s/n, Ciudad Universitaria, CP 04510 Mexico Distrito Federal, Mexico*
9 *Dept. of Physics and Geology, Northern Kentucky University, Highland Heights, KY 41099, USA*

The Cosmic-Ray Energetics And Mass (CREAM) instrument for the International Space Station (ISS) is a detector for studying the origin, acceleration and propagation mechanism of high-energy cosmic rays. The ISS-CREAM instrument is scheduled to launch in 2017 to the ISS. The Top and Bottom Counting Detectors (TCD/BCD) are designed for studying electron and gamma-ray physics. The TCD/BCD are composed of a plastic scintillator and an array of photodiodes The active detection areas of the TCD/BCD are 500 $\times$ 500 mm^2 and 600 $\times$ 600 mm^2, respectively. The TCD/BCD were completed in 2015 and passed the environmental tests for safety in a space environment. After finishing these tests, the TCD/BCD were integrated with the payload. The TCD is located between the carbon target of the ISS-CREAM instrument and the calorimeter, and the BCD is located below the calorimeter. The TCD/BCD can distinguish between electrons and protons by using the different shapes between electromagnetic and hadronic showers in the high-energy region. We study the TCD/BCD performance in various energy ranges by using GEANT3 simulation data. Here, we present the status of the electron and proton separation study with the TCD/BCD simulation.

35th International Cosmic Ray Conference
10-20 July, 2017
Bexco, Busan, Korea

PoS(ICRC2017)250

1. Introduction

The ISS-CREAM detector will be launched in August 2017 to ISS. The ISS-CREAM detector can measure cosmic rays from 10 GeV to > 100 TeV [1]. It is expected that measurements of high energy cosmic-rays provides a key to understanding the origin and propagation of cosmic rays [2].

The ISS-CREAM detector is composed of five sub-detectors as shown in Figure 1. The Silicon Charge Detector (SCD) is located at the top of the ISS-CREAM detector and the Top Counting Detector (TCD) is placed under the carbon targets. The sampling Calorimeter (CAL) is between the TCD and the Bottom Counting Detector (BCD). The Boronated Scintillator Detector (BSD) is located at the bottom of the ISS-CREAM detector.

It is important to separate protons and electrons in the cosmic-ray spectrum for studying the electron spectrum. Since protons are the dominant component in cosmic rays [3]. The TCD/BCD can separate them by using the difference between electromagnetic and hadronic showers. The TCD/BCD also provide a redundant trigger in addition to the CAL trigger and a low- energy electron trigger. In this paper, the TCD/BCD and e/p separation studies using GEANT3 simulations are described.

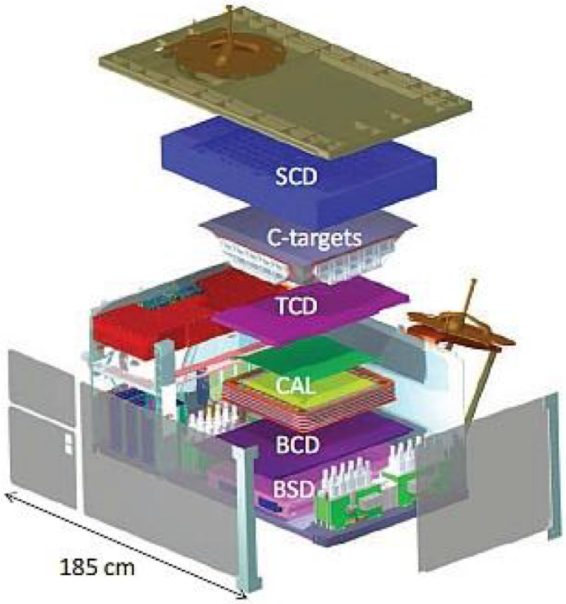

Figure 1: Schematic of the ISS-CREAM instrument, composed of a SCD, carbon target, TCD/BCD, CAL and BSD [4].

*Speaker.
†Email: sinchul1216@gmail.com
‡Currently at Korea Atomic Energy Research Institute, Gyeongju 38180, Republic of Korea
§Currently at Pohang Accelerator Laboratory, Pohang 37673, Republic of Korea
¶Currently at Advanced Radiation Technology Institue, Korea Energy Research Institute, Jeongup 56212, Republic of Korea

2. Top and Bottom Counting Detectors

The TCD is located between the carbon target and the CAL, and the BCD is located below the CAL as shown in Figure 1. The dimensions of the TCD are 901 $\times$ 551$\times$ 30 mm^3 and those of the BCD are 950 $\times$ 650 $\times$ 33 mm^3 as shown in Figure 2. Each of the TCD/BCD consists of a plastic scintillator and 20 $\times$ 20 silicon photodiode array. The dimensions of the plastic scintillators for the TCD and BCD are 500 $\times$ 500 $\times$ 5 mm^3 and 600 $\times$ 600 $\times$ 10 mm^3, respectively. The dimensions of the silicon photodiode are 23 mm $\times$ 23 mm $\times$ 650 μm. The plastic scintillator is attached to the silicon photodiodes by using DC 93-500 optical silicone adhesive (Dow Corning), and the silicon photodiode is attached to a printed circuit board by using Eccobond 56 C conductive epoxy (Hysol) [5].

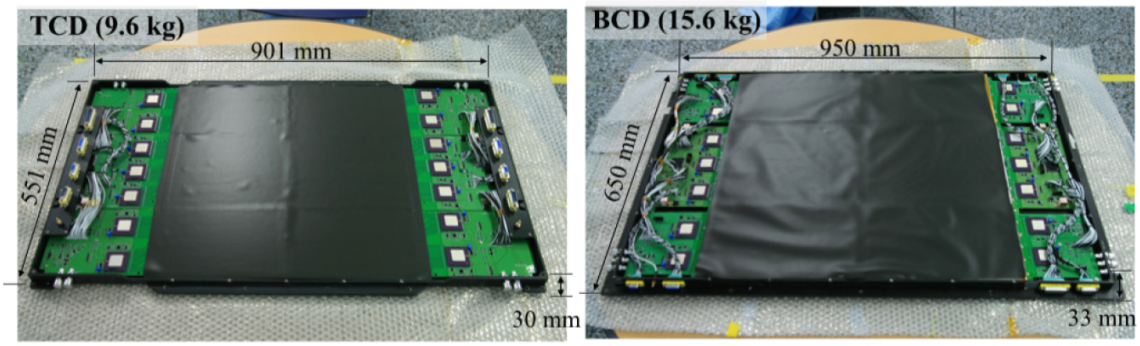

Figure 2: Assembled TCD (left) and BCD (right) before insertion into their mechanical enclosures [5].

The TCD/BCD electronics are composed of two motherboards and four daughter boards for each TCD/BCD as shown in Figure 3. Each motherboard has three VA-TA chips [5], an ACTEL chip and two DC-DC converters. Each daughter board has two VA-TA chips to read the signals.

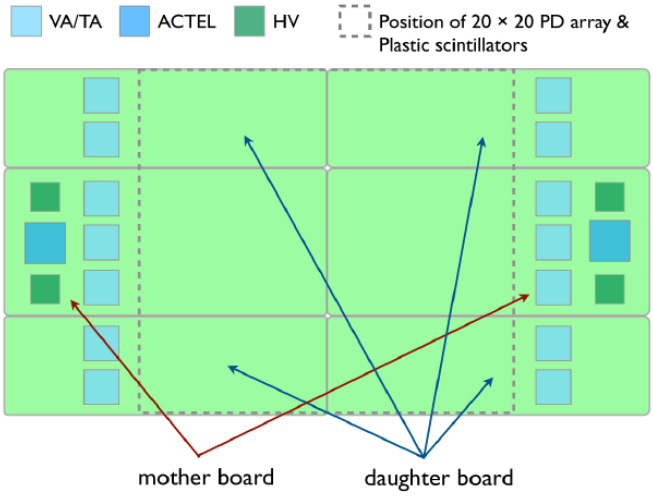

Figure 3: Design of the TCD/BCD electronics. There are two motherboards and four daughter boards for each of the TCD and the BCD [6].

The TCD/BCD are designed for measuring scintillation light produced when cosmic rays pass through the plastic scintillator. The silicon photodiode converts the scintillation light from the the plastic scintillator into an electric current, and also produces electron-hole pairs when the cosmic rays pass through. As shown in Figure 4, the CAL is placed between TCD and BCD. Thus the TCD/BCD can measure the shower shape of cosmic rays before and after they pass through the CAL.

3. e/p Separation Study using the GEANT3 Simulation

The TCD/BCD separate electrons and protons using the different shower shapes between electro magnetic and hadronic showers. In this study, GEANT3 simulations are used to study the separation between electrons and protons in various energy regions. In each energy region, 10,000 electrons and protons are produced using the GEANT3. A Boosted Decision Tree (BDT) [7] analysis with the shower width in the TCD/BCD, the number of hits in the TCD/BCD, the deposited energy in the TCD/BCD, and the deposited energy in the CAL are used for separating electrons from protons. The Toolkit for Multi Variable Analysis (TMVA) [7] is used to train and test the BDT, and we used ROOT [8] for data analysis.

3.1 Energy Distribution in the CAL

To distinguish between electrons and protons, we first use the distribution of deposited energy in the CAL. The energy distribution of electron is fitted using an asymmetric gaussian function. Then, the energy range of the 2σ region is determined. We select the particles which deposited the energy in the corresponding range. Figure 5 shows the deposited energy distribution of 300 GeV electrons in the CAL with asymmetric gaussian fit. The mean value is 1.295 GeV, σ_{left} is 0.047 GeV and σ_{right} is 0.071 GeV. We selected the particles with deposited energy between 1.201 GeV and 1.437 GeV in the CAL for the 300 GeV electron.

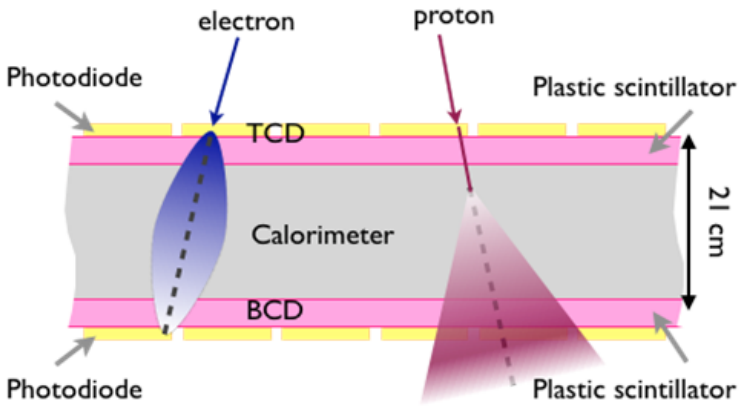

Figure 4: Schematics of the particle shower generated when electrons and protons pass through the TCD/BCD [6].

3.2 e/p Separation using the BDT

The BDT is one of the multivariable methods. A decision tree is a sequence of binary splits of the data. Repeated decisions are made on one single variable at a time until a stop criterion is fulfilled. There are several popular criteria to determine the best particle identification variable and best place on which to split a node. In this study, the gini criterion [9] is used. Decision trees are powerful, but not stable. A small fluctuation in the data can make a large difference in the tree. This can be improved by the use of boosting. For boosting, the training events which were misclassified have their weights increased, and a new tree is formed. This procedure is then repeated for the new tree. In this way many trees are built up. There are many methods to boost a BDT. In this study, the AdaBoost process [7] is used.

To make the BDT, the variables such as energy in the CAL, shower distribution in the TCD/BCD (RMS^2 and f-factor), the number of hits in the TCD/BCD, and deposited energy in the TCD/BCD are used. The RMS^2 is defined as

$$RMS^2 = E_{TCD_i} \times (x_i - x_c)^2 + (y_i - y_c)^2. \tag{3.1}$$

where E_{TCD_i} is the deposited energy in the ith photodiode in the TCD, x_i and y_i are the coordinates of the center of the energy deposited in the photodiode sensors, and x_c and y_c are the coordinates of the energy center in the TCD_i. The f-factor is defined as

$$f\text{-}factor = RMS^2 \times E_{BCD}/E_{CAL}. \tag{3.2}$$

where E_{BCD} is the deposited energy in the BCD and E_{CAL} is the deposited energy in the CAL. These two criteria are similar to those of the ATIC analysis methods [10]. We trained and tested BDT

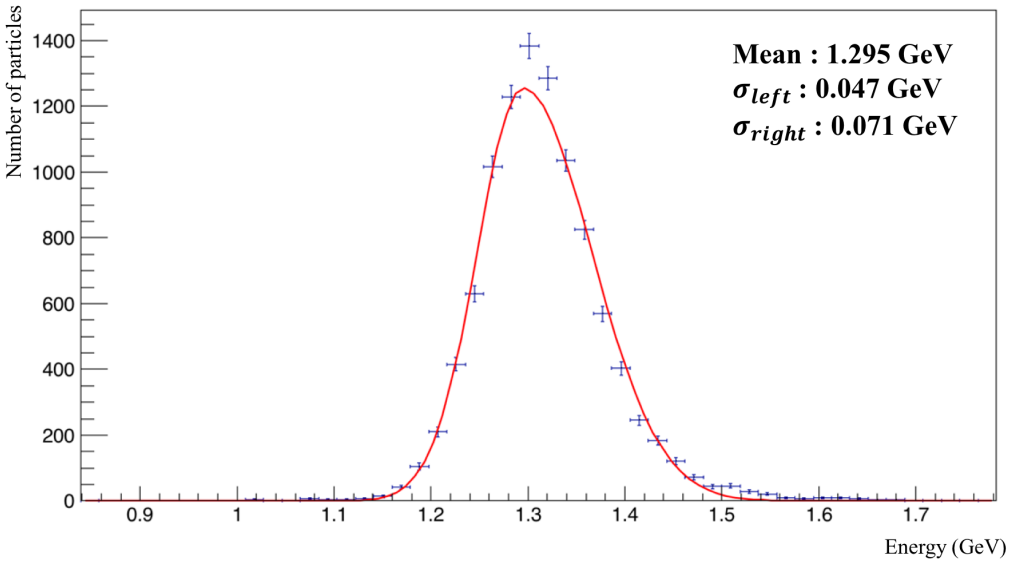

Figure 5: The distribution of deposited energy in the CAL by 300 GeV electrons. The distribution is fitted using an asymmetric gaussian function. The mean value is 1.295 GeV, σ_{left} is 0.047 GeV and σ_{right} is 0.071 GeV.

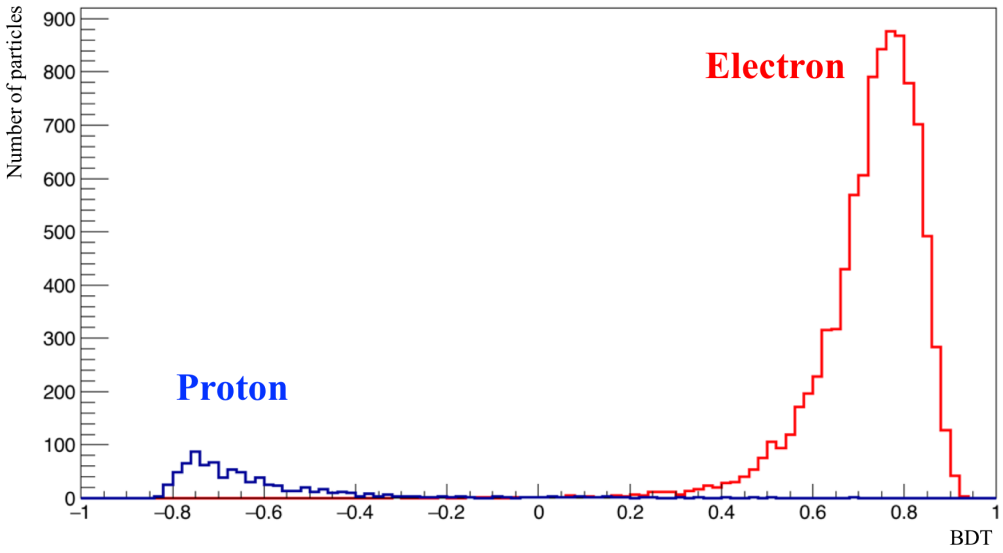

Figure 6: The BDT output distribution for 300 GeV electron and 900 GeV proton. The red line is for electron events and the blue one is for proton events. The events considered to be electrons are close to 1 and those considered to be protons are close to -1.

in each energy region. The Figure 6 shows the BDT result when electron energy is 300 GeV and proton energy is 900 GeV. Since many proton events are rejected in the cut using the deposited energy in the CAL, the number of protons is smaller than the electrons. Table 1 is shows the proton rejection power and electron efficiency when BDT is larger than 0. The electron efficiency is about 93% and the proton rejection power is increased with increasing the energy

4. Conclusions

The ISS-CREAM detector will be launched to the ISS in August 2017. The ISS-CREAM detector will measure cosmic rays from 10 GeV to 100 TeV and expects to obtain information on their source and propagation.

Since the cosmic-ray protons account for most of the primary cosmic rays, and the absolute charges of a proton and an electron are the same, it is necessary to distinguish between protons and electrons to study the cosmic-ray electrons. The TCD/BCD can separate the protons and electrons by measuring the shower profile before and after passing through the CAL. The difference between electromagnetic and hadronic showers can be used to distinguish between electrons and protons.

In this study, we get a proton rejection power in various energy regions using GEANT3 simulation. The BDT method is used for separating electrons and protons. The variables for the analysis are the deposited energy in the CAL, the shower width in the TCD/BCD, the number of hits in the TCD/BCD, and the deposited energy in the TCD/BCD.

The electron efficiency obtained in this study is about 93%, and the proton rejection power is increased with increasing energy. The work is ongoing to study the proton rejection power and electron efficiency by generating electrons and protons according to the cosmic-ray spectrum.

Table 1: Electron efficiency and proton rejection power in each energy region. The total number of generated electrons and protons is 10,000.

Energy (GeV)	Accepted electron	Selected proton	Electron efficiency (%)	Proton rejection power
30	9439	92	94.4 ± 0.2	$(1.03 \pm 0.11) \times 10^2$
50	9442	61	94.4 ± 0.6	$(1.55 \pm 0.20) \times 10^2$
70	9434	51	94.3 ± 0.5	$(1.85 \pm 0.26) \times 10^2$
120	9406	44	94.1 ± 0.4	$(2.14 \pm 0.32) \times 10^2$
150	9436	35	94.4 ± 0.4	$(2.70 \pm 0.46) \times 10^2$
300	9335	31	93.3 ± 0.3	$(3.01 \pm 0.54) \times 10^2$
900	9276	14	92.8 ± 0.1	$(6.6 \pm 1.8) \times 10^2$
1,200	9239	11	92.4 ± 0.1	$(8.4 \pm 2.5) \times 10^2$
2,500	9246	9	92.5 ± 0.1	$(1.03 \pm 0.34) \times 10^3$
5,000	9218	8	92.2 ± 0.1	$(1.15 \pm 0.41) \times 10^3$
10,000	9195	8	92.0 ± 0.1	$(1.15 \pm 0.41) \times 10^3$

Acknowledgments

The authors thank the NASA GSFC WFF for project management and engineering support, and NASA JSC ISS Program Office for launch support and the ISS accommodation. This work was supported in the U.S. by NASA grants NNX11AC52G, NNX08AC15G, NNX08AC16G and their predecessor grants, as well as by directed RTOP funds to NASA GSF WFF. It is supported in Korea by the Creative Research Initigatives of MEST/NRF and by National Research Foundation Grants NRF-2014R1A2A2A01002734, NRF-2014R1A1A2006456, NRF-2015R1A2A1A13001843. It was supported in France by IN2P3/CNRS and CNES and in Mexico by DGAPA-UNAM and CONACYT. The authors also thank H.S. Choi, Korea Instute of Industrial Technology, for contributions to the SCD thermal vacuum test, M. Geske, Penn State, for contributions to the BSD, and M.A. Coplan, University of Maryland, contributions to CAL electronics vacuum tests.

References

[1] E.S. Seo et al., Adv. Space Res. **53**, No. 10, 1451 (2014).

[2] O. Adriani et al., Phys. Rev. Lett. **106**, 201101 (2011).

[3] R.A. Mewaldt, Adv. Space Res. **14**, No. 10, 737 (1994).

[4] E.S. Seo et al., In *Proceeding of the 33rd ICRC*, p. 629 (2013).

[5] J.M. Park et al., In *Proceeding of the 34th ICRC* (2015).

[6] H.Y. Hyun et al., In *Proceeding of the 33rd ICRC*, p. 2017 (2013).

[7] P. Speckmayer et al., J. Phys.:Conf. Ser. 219, 032057 (2010)

[8] R. Brun and F. Rademakers, Nucl. Instrum. Methods Phys. Res., Sect. A 389, 81 (1997).

[9] Byron p. Roe, H.J. Yang and J. Zhu, In *Proceeding of PHYSTAT05*, p. 12 (2005).

[10] J. Chang et al., Adv. Space Res. **42**, 431 (2008).